Changes in Molecular Weights and Molecular Weight Distributions of Differently Stranded Nucleic Acids after Sonication: Gel Permeation Chromatography/Low Angle Laser Light Scattering Evaluation and Computer Simulation†

Masato Tanigawa,*,‡ Masashi Suzuto, Kiyohiro Fukudome, and Kiwamu Yamaoka*

Department of Materials Science, Faculty of Science, Hiroshima University, 1-3-1 Kagamiyama, Higashi-Hiroshima 739, Japan

Received March 11, 1996; Revised Manuscript Received August 15, 1996⊗

ABSTRACT: Changes of weight-average molecular weights (M_w) and the molecular weight distributions in terms of weight fraction (g_w) were evaluated in the course of sonication for three nucleic acids in different conformations by the gel permeation chromatography/low angle laser light scattering (GPC/LALLS) method. High M_w samples used were single-stranded poly(uridylic acid), $(U)_n$, double-stranded DNA, and triple-stranded poly(adenylic acid)·2poly(inosinic acid), $(A)_n·2(I)_n$, in 0.2−0.1 M NaCl at 0 °C. The experimental g_w vs M curves were computer-simulated for different chain-scission mechanisms: (1) random, (2) midpoint, (3) Gaussian, (4) classical partially random, and (5) newly proposed partially random scission models. In comparison with the GPC/LALLS data, the middle portion of each single- or multiple-stranded chain was sheared randomly, whereas the adjacent end portions of the chain resisted sonic scission. The M_w value of each intact end portion was 1.0×10^5 for $(U)_n$, 1.5×10^5 for DNA, and 1.7×10^5 for $(A)_n·2(I)_n$, corresponding to the lowest possible M_w for the sonicated but unfractionated nucleic acid samples under the present conditions.

Introduction

High molecular weight intact DNA samples are known to be degraded to smaller size fragments by the ultrasonic irradiation without their double-helical conformation being ruptured, if a proper sonication procedure is adopted.[1−15] This is indeed a well-established and convenient technique to prepare fairly large quantities of DNA with various molecular weights for physicochemical studies in solutions.[14,15] Among them are, for example, the molecular weight dependence of light scattering,[1,16] viscosity,[5,16,17] circular dichroism,[18] and electric linear dichroism,[19] to name a few. By carefully fractionating sonicated fragments, the well-characterized fractions of lower molecular weight can be prepared not only for double-helical DNA but also for other nucleic acids such as triple-stranded synthetic polynucleotides. In addition, the molecular weight distribution curve and degree of polydispersity of these sonicated polymers can now be evaluated quantitatively by the gel permeation chromatography/low angle laser light scattering (GPC/LALLS) method.[17,20]

The degradation of various kinds of polymers has been studied, by using both theoretical[21−30] and experimental[31−33] methods; for example, Heymach and Jost[29] calculated the change in molecular weight distribution of the polymer chain in cases of random and restricted shearings. Using a computer simulation technique, Ballauf and Wolf[30] could reproduce the change of the molecular weight and the molecular weight distribution of polystyrene on the assumption that the molecular weight distribution of the polymer prior to degradation can be expressed by the Schulz−Zimm distribution function.[34] They calculated the degradation process on the basis of three (the random, midpoint, and Gaussian) scission models and showed the relation between the mechanism and the change of molecular weight distribution. Nevertheless, the probability of scission upon ultrasonic irradiation still remains to be clarified for actual polymer systems.

In the present work, changes in molecular weight and the distribution were experimentally studied by the GPC/LALLS method for three nucleic acids of different types in the course of ultrasonic irradiation. The high molecular weight samples, i.e., the double-stranded helical DNA, a single-stranded random-coiled poly(uridylic acid), $(U)_n$, and a triple-stranded helical poly(adenylic acid)·2poly(inosinic acid), $(A)_n·2(I)_n$, were chosen to ascertain the effect of sonication on the chain rigidity and to compare the presently observed data with those previously reported for other multistranded polynucleotides with different constituent bases.[17,20] Calculations were performed for various scission models with the objective for clarifying the effect of sonication process on the change of molecular weight distribution. Finally, a plausible sonication mechanism was proposed for each nucleic acid, by comparing computer-simulated results with experimental observations.

Experimental Section

Materials and Preparations. High molecular weight calf thymus DNA ($M_w \doteqdot 8 \times 10^6$) was purchased from Worthington Biochemical Corp. (lot. no. X9J1174). The stock solution was prepared, by dissolving it in 0.2 M NaCl. High molecular weight polyribonucleotide samples were all purchased from

† Ultrasonic Scission of Deoxyribonucleic Acid in Aqueous Solution. 8. Part 7 of this series, ref 20.

* Author to whom correspondence should be addressed.

‡ Present address: Joint Research Center for Atom Technology, Angstrom Technology Partnership, 1-1-4 Higashi, Tsukuba, 305, Japan.

⊗ Abstract published in *Advance ACS Abstracts,* October 1, 1996.

S0024-9297(96)00370-1 CCC: $12.00

Yamasa Shoyu Co., Ltd. (Choshi, Japan). The stock solution of single-stranded $(U)_n$ with an M_w of 3.1×10^5 (lot no. 401078, $S_{20,w} = 6.1$) was prepared, by dissolving it in 0.2 M NaCl. $(A)_n$ (lot no. 101077, $S_{20,w} = 8.0$) and $(I)_n$ (lot no. 501476, $S_{20,w} = 9.6$) were mixed at a 1:2 molar ratio and incubated at 7 °C for 2 days at a pH of 7.4 in sodium phosphate buffer containing 0.4 M NaCl to prepare a high molecular weight triple-stranded $(A)_n \cdot 2(I)_n$ helix. The preparation, characterization, and solution properties of the $(A)_n \cdot 2(I)_n$ helix will be reported elsewhere.[35]

Ultrasonic Irradiation. Ultrasonic irradiation was carried out with a Tomy sonicator, Model UD-200P (Tomy Seiko Co., Tokyo), at an output power level of 200 W (20 kHz) for 20 min for DNA and $(A)_n \cdot 2(I)_n$ (40 repetitions of a 30-s burst and subsequent 5-min bubbling interval cycle) and 30 min for $(U)_n$ (60 repetitions of the same cycle) under a helium atmosphere. A 70−120-mL polymer solution (2 mg/mL) was placed in a three-way branched rosette vessel of about 150 mL in volume, which enabled vigorous circulation of the content by jet flows for rapid temperature equilibration. Into the vessel, which was held at 0 °C in an iced bath, the helium gas was introduced for 15 min before sonication to expel the dissolved air. The sonication procedure has been described elsewhere in detail.[15] Possible damage to the irradiated nucleic acid bases and the strand separation of DNA or $(A)_n \cdot 2(I)_n$ were checked with the UV absorption spectra of each polymer solution before and after sonication. No anomaly was detected in the spectra.

GPC/LALLS. Each solution was sampled intermittently in the course of sonication. The molecular weight and distribution pattern were determined at 30 °C on a Tosoh flow-type GPC/LALLS apparatus (Tosoh Co., Tokyo), which consists of two Tosoh TSK G-DNA-PW columns in tandem, a Tosoh LS-8000 light scattering photometer, and a Tosoh RI-8011 differential refractometer. For each typical run, a sample solution (0.5 mL) was injected into a sample loop and eluted with 0.2 M NaCl eluent at a flow rate of 0.6 mL/min. The solvent was filtered through a sintered stainless filter before injection to the GPC column and then through a 0.45-μm pore size cellulose acetate membrane (Millipore Co., HAWP 01300) in front of the LALLS apparatus for complete removal of dusts. Details were given in previous papers from this laboratory.[17,20] A bovine serum albumin sample (molecular weight = 66 250) from Miles Inc., Diagnostics Div., and a chicken erythrocyte nucleosomal DNA sample (molecular weight = 95 700) were used as the molecular weight standards.

The weight fraction $f_w(M)$ for molecules with the molecular weight M can be evaluated from the ratio of light scattering intensity to refractive index intensity. In order to visualize the molecular weight distribution over a wide range of M, another weight fraction should be used. It is defined as $g_w(\log M)$, which is the function of log M:

$$f_w(M)\,\mathrm{d}M = f_w(M)\left(\frac{\mathrm{d}M}{\mathrm{d}\log M}\right)\mathrm{d}\log M \equiv g_w(\log M)\,\mathrm{d}\log M \tag{1}$$

Hence, the molecular weight distribution can finally be calculated and represented as the g_w vs log M curve.

Computational Section

Procedure for Calculation. The present calculation was performed in a manner similar to the procedure proposed by Ballauf and Wolf.[31] Let the molecular weight distribution of polymer chains at time t be given by $\mathbf{F}(t)$; then, the change in molecular weight distribution with a lapse of sonication time t is expressed as

$$\frac{\mathrm{d}}{\mathrm{d}t}\mathbf{F}(t) = \mathbf{A}\mathbf{F}(t) \tag{2}$$

$$\mathbf{F}(t) = \begin{pmatrix} f(1,t) \\ f(2,t) \\ \cdot \\ \cdot \\ f(i,t) \\ \cdot \\ \cdot \\ f(201,t) \end{pmatrix}$$

$$\mathbf{A} = \begin{pmatrix} a(1,1) & a(1,2) & \cdots & a(1,j) & \cdots & a(1,201) \\ a(2,1) & a(2,2) & \cdots & \cdot & \cdots & \cdot \\ \cdot & \cdot & \cdots & \cdot & \cdots & \cdot \\ \cdot & \cdot & \cdots & \cdot & \cdots & \cdot \\ a(i,1) & \cdot & \cdots & a(i,j) & \cdots & \cdot \\ \cdot & \cdot & \cdots & \cdot & \cdots & \cdot \\ \cdot & \cdot & \cdots & \cdot & \cdots & \cdot \\ a(201,1) & \cdot & \cdots & \cdot & \cdots & a(201,201) \end{pmatrix} \tag{3}$$

where $f(i,t)$ is the number fraction of polymer molecules, each consisting of i segments at an irradiated time t; the element $a(i,j)$ of matrix $\mathbf{A}$ expresses the scission probability of a polymer molecule with j segments into two fragments with i and $j - i$ segments; and the diagonal element $a(j,j)$ is the scission probability of the polymer molecule with j segments into fragments with arbitrary segments. The diagonal element $a(j,j)$ is given as

$$a(j,j) = -\sum_{i=1}^{j-1}\frac{a(i,j)}{2} \tag{4}$$

It should be noted that the matrix $\mathbf{A}$ has a triangular form. With computer-aided iterative calculations, the change of molecular weight distribution with the lapse of time t can be evaluated in the course of a sonication process.

Actual calculations were performed on EPSON PC-386VR and NEC PC9801FA computers. The input data were the molecular weight distribution, determined by the GPC/LALLS method, for each high molecular weight sample. The assumption was made that the longest molecule in a given polymer system is composed of 201 identical segments. The number fraction of molecules with a particular number of segments was calculated by the Spline interpolation method. On the basis of the different models, which are shown in the following section, 201 simultaneous first-order differential equations were set up for changes of the number fraction of molecules with various segments with time t. These differential equations were solved successively by the Milne method for evaluating the molecular weight distribution in terms of the number fraction of molecules with molecular weight M, $f_n(M)$, in the course of sonication. This number fraction at time t was converted to the weight fraction, $f_w(M)$, and finally the molecular weight distribution was presented in term of the $g_w(\log M)$ vs log M plot.

Models for the Scission Process. Computer-simulations were performed with the following five models. In the first three models, the scission probability is proportional to molecular weight or length.

1. Random Scission Model I. In this model, the chain scission occurs randomly at any site on a chain with an equal probability. The scission probability is

expressed as

$$a(i,j) = c \quad (i \le j)$$
$$a(i,j) = 0 \quad (i > j) \tag{5}$$

where c is a constant.

2. Midpoint Scission Model II. In this model, a polymer chain is sheared only at the midpoint. The scission probability is expressed as

$$a\left(\frac{j}{2},j\right) = cj$$
$$a\left(\frac{j}{2}+1,j\right) = cj \tag{6}$$
$$a(i,j) = 0 \quad \left(i \neq \frac{j}{2}, \frac{j}{2}+1\right)$$

where c is a constant.

3. Gaussian Scission Model III. In this model, the probability of scission is expressed by a Gaussian function, being the largest at the center of each chain, and is expressed as

$$a(i,j) = c \exp\left\{-\frac{2}{2\sigma^2}\left(i-\frac{j}{2}\right)^2\right\} \quad (i < j)$$
$$a(i,j) = 0 \quad (i > j) \tag{7}$$

where c is a constant and σ is the standard deviation of the Gaussian function being set equal to $0.2i$ in this calculation.

4. Classical (Partially Random) Scission Model IV. In this model, a polymer chain is utterly resistant to shearing in the vicinity of both ends. Except for the end region, the polymer chain is sheared at random. Therefore, the scission probability is expressed as

$$a(i,j) = 0 \quad (i \le k_0, j-k_0 \le i \le j-1)$$
$$a(i,j) = c \quad (k_0 < i < j-k_0) \tag{8}$$
$$a(i,j) = 0 \quad (i > j)$$

where c is a constant and k_0 is the number of segments in a molecule. If $k_0 = 0$, this model reduces to (random scission) model I. A chain composed of segments less than k_0 remains unaffected.

5. Newly Proposed Scission Model V. This model is an extension of classical scission model IV. In model V, the scission probability is nonzero anywhere on a chain. However, the chain is hardly scissile in the vicinity of the ends. Scission takes place randomly anywhere in the central region of the chain. The scission probability is expressed as

$$a(i,j) = c\left[1-\exp\left\{-\left(\frac{i}{k_0}\right)^n\right\}\right] \quad \left(i \le \frac{j}{2}\right)$$
$$a(i,j) = c\left[1-\exp\left\{-\left(\frac{201-i}{201-k_0}\right)^n\right\}\right] \quad \left(\frac{j}{2} \le i \le j-1\right) \tag{9}$$
$$a(i,j) = 0 \quad (i > j)$$

where c is a constant. If $k_0 = 0$, this model reduces to random scission model I. If the exponent n is infinitely large, this model is in agreement with the classical scission model IV. Thus, the presently proposed model (V) contains two previous models as the limiting case.

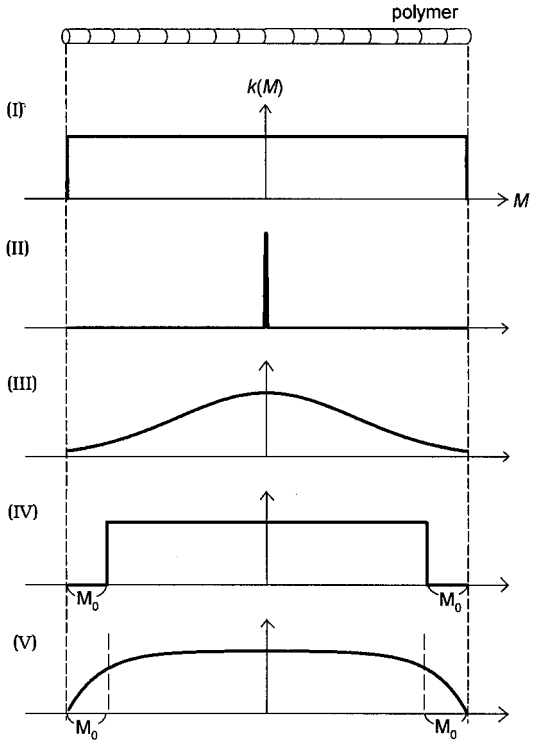

Figure 1. Models for the scission probability: (I) random scission model, (II) midpoint scission model, (III) Gaussian scission model, (IV) classical scission model, and (V) newly proposed scission model. The ordinate is the scission probability $k(M)$, in which M is the distance from the end of a polymer chain in terms of molecular weight; M_0 stands for the unsonicated end region.

Figure 1 shows schematically the scission probability of a chain on the basis of these five scission models, I−V.

Results and Discussion

Experimentally Determined M_w and g_w vs M. The Case of DNA. Figure 2 shows the change in molecular weight distribution of a high molecular weight DNA, hDNA ($M_w = 8.3 \times 10^6$), in the course of sonication time (t) in terms of the weight fraction, g_w, of sheared fragments versus molecular weight (M). Dotted curves indicate the GPC/LALLS-determined experimental $g_w(\log M)$ vs $\log M$, which is simply denoted hereafter as g_w vs M. The lapse of sonication time (in the direction of the arrow) makes the average molecular weights of sonicated fragments lower and the corresponding distributions narrower. The behavior of sonication can now be revealed quantitatively in this work, though similar results have been cited occasionally on a qualitative basis.[2,23,30] Since the molecular weight of the original hDNA sample is too large and beyond the exclusion limit of the GPC column (Tosoh TSK G-DNA-PW), the g_w vs M curve cannot be evaluated accurately by the GPC/LALLS method. In this work, therefore, only the M_w value could be estimated from the ratio of the total intensity of light scattering to that of refractive index, as indicated with a dashed vertical line (Figure 2a). Successive changes of the g_w vs M curves show that even the initial shortest burst time (no. 1, 30 s) reduces the M value nearly 10-fold; M values approach steadily to a low molecular weight limit (no. 9, 20 min) with narrower distributions after prolonged sonication periods. Figure 2b−e show quantita-

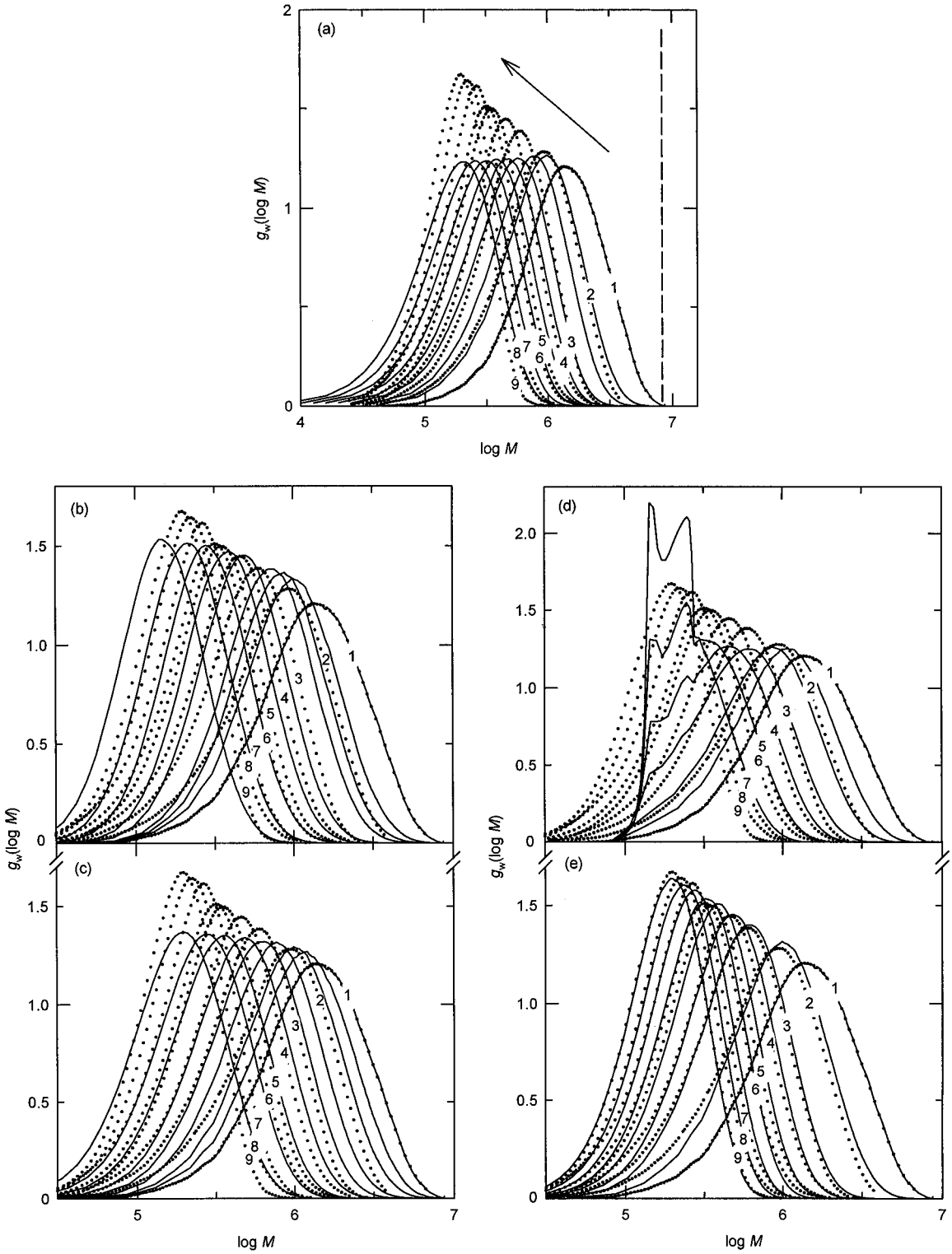

Figure 2. Measured and simulated molecular weight distributions of DNA in the sonication process: Dotted curves, GPC/LALLS-determined experimental molecular weight distributions (a−e). Irradiation time in min: (1) 0.5, (2) 1.0, (3) 2.0, (4) 3.0, (5) 4.5, (6) 6.5, (7) 9.5, (8) 13.5, (9) 20. Solid lines are simulated molecular weight distributions: (a) random scission model calculated with eq 5, (b) midpoint scission model (eq 6), (c) Gaussian scission model (eq 7), (d) classical scission model (eq 8), (e) newly proposed scission model (eq 9). The ordinate is the weight fraction $g_w(\log M)$, in which M is the molecular weight. The dashed vertical line in (a) is the M_w of hDNA.

tive comparisons between experimental data (dotted) and theoretical calculations (solid) for different sonication mechanisms (vide post).

Figure 3 shows the dependence of M_w on irradiation time (circles in upper half) and the degree of polydispersity, expressed in terms of the ratio of the weight-average to number-average molecular weights (M_w/M_n), on the time (circles in lower half). In this figure, the initial 30-s burst sample is taken as the original ($M_w = 1.7 \times 10^6$ and $M_w/M_n = 1.8$), instead of the unsonicated hDNA, for which the M_w/M_n value could not be available from GPC/LALLS. For an accumulated period of 20-min irradiation, the molecular weight is reduced to 2.0×10^5, more than 40-fold reduction, as compared with the original M_w of hDNA. Similarly, the polydispersity parameter M_w/M_n is also decreased from 1.8 to 1.4 after

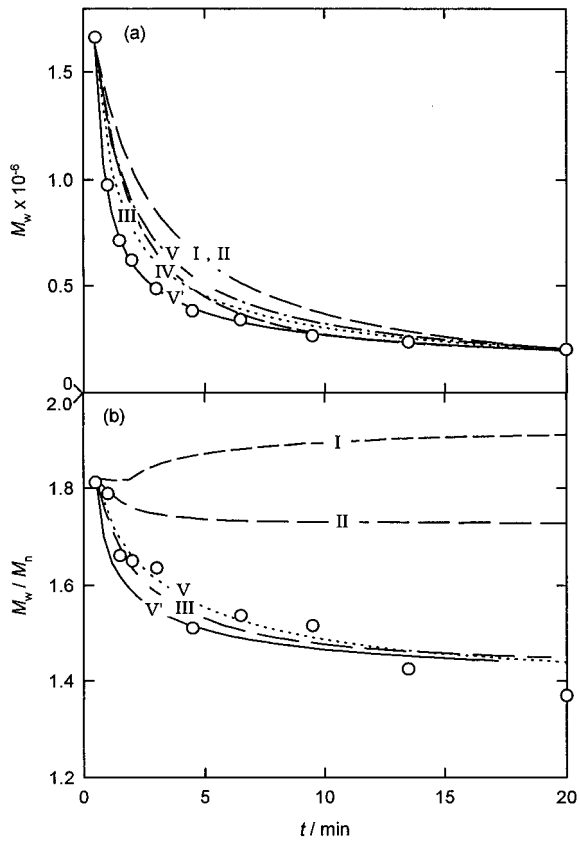

Figure 3. Dependence of the weight-average molecular weight M_w (a) and the ratio of the weight- to number-average molecular weight (M_w/M_n) (b) on ultrasonic irradiation time. Circles are measured values. Each lined curve was calculated on the basis of sonication mechanisms of the random scission model (I), midpoint scission model (II), Gaussian scission model (III), classical scission model (IV), newly proposed scission model (V), and modified newly proposed scission model (V′). In b model IV behaved abnormally.

a 20-min sonication. These two facts, now verified, have been taken qualitatively into account in the past in the preparation of low molecular DNA samples for conformational and other solution studies.[14,35]

The Case of $(U)_n$. Figure 4a shows the observed changes of the molecular weight distribution (dotted curves) of $(U)_n$ sampled out in the course of sonication. The unsonicated $(U)_n$ sample is successively sheared to shorter fragments after a lapse of 30-min sonication with narrower molecular weight distributions. Figure 4b shows the dependence of M_w and M_w/M_n on sonication time; the values are reduced from 3.1×10^5 to 6.4×10^4 and from 1.7 to 1.2 after a lapse of 30 min, respectively. These parameters are all affected strongly at the initial 5−6-min period after the start of sonication, as also observed for DNA. The result in Figure 4 indicates that the present sonication procedure can also be utilized effectively to prepare a single-stranded polynucleotide of random-coiled conformation with reasonably low molecular weight and molecular weight distribution.

The Case of $(A)_n \cdot 2(I)_n$. Figure 5a shows observed changes of the molecular weight distribution (dotted curves) of $(A)_n \cdot 2(I)_n$ with sonication time. The M_w value of the unsonicated sample is too large to be subjected to the GPC/LALLS determination due to the same reason as hDNA. The distribution profiles at the initial irradiations are broad and skewed toward smaller molecular weight fragments (e.g., no. 1, 1 min). Interestingly, however, the pattern of skew reverses, now

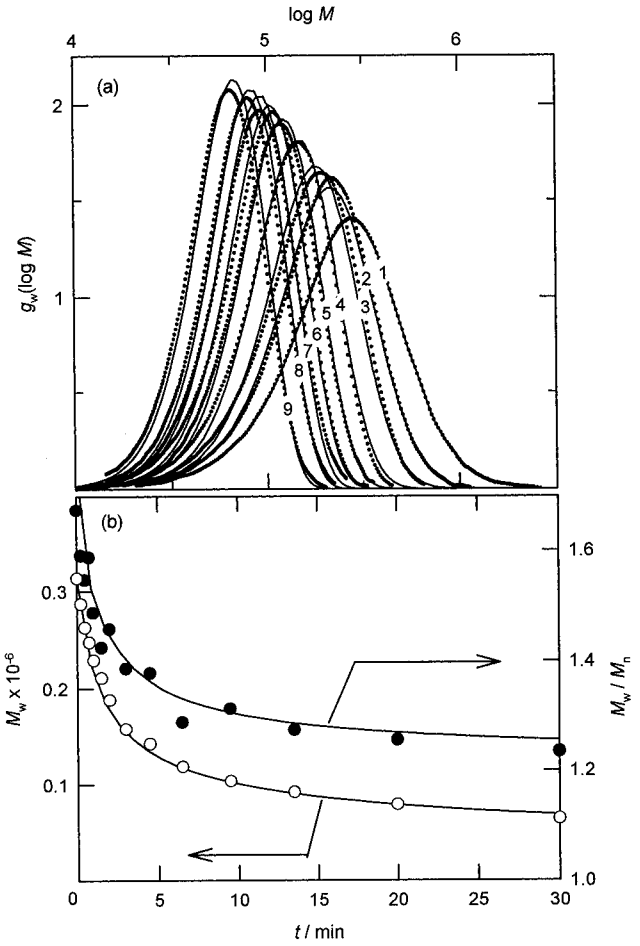

Figure 4. (a) Measured and simulated molecular weight distributions and (b) changes of the weight-average molecular weight M_w and the degree of polydispersity M_w/M_n in the ultrasonic irradiation process for $(U)_n$. (a) Dotted curves, are the GPC/LALLS-determined experimental molecular weight distributions. Irradiation time in min: (1) 0, (2) 1, (3) 2, (4) 4.5, (5) 6.5, (6) 9.5, (7) 13.5, (8) 20, (9) 30. Solid lines are the simulated molecular weight distributions based on model V. The weight fraction $g_w(\log M)$ was plotted against the logarithm of molecular weight log M. (b) Circles are experimental values, M_w (○) and M_w/M_n (●), solid lines are simulated on the basis of the modified newly proposed scission model (V′).

tailing toward higher molecular weight fragments, as the sonication time proceeds. Figure 5b shows the dependence of M_w (open circles) and M_w/M_n (filled circles) values for $(A)_n \cdot 2(I)_n$ fragments on the sonication time. The initial 5-min irradiation time appears to be sufficient to reduce the M_w value by ca. 4-fold. At the same time, the broad distribution of the unsonicated sample rapidly becomes narrower at an early stage of sonication. Although the triple-stranded $(A)_n \cdot 2(I)_n$ is an unusual purine-purine helix, it can also be sonicated to shorter fragments; thus, a large quantity can be prepared to serve for many physicochemical studies in solution.[36] This sonication behavior is in accord with a previous report on other triple-stranded helices more commonly available.

Susceptibility of Different Strands to Sonication. The weight-average degree of polymerization, DP_w, may be expressed by dividing the M_w value of a given nucleic acid by the average monomeric unit, i.e., 328 for $(U)_n$, 660 for DNA, and 1055 for $(A)_n \cdot 2(I)_n$. In order to compare the susceptibility of these nucleic acids to ultrasonic scission, the data in Figures 3a, 4b, and 5b are all replotted, by adjusting the coordinates so that the sonication starts for the samples with the same DP_w

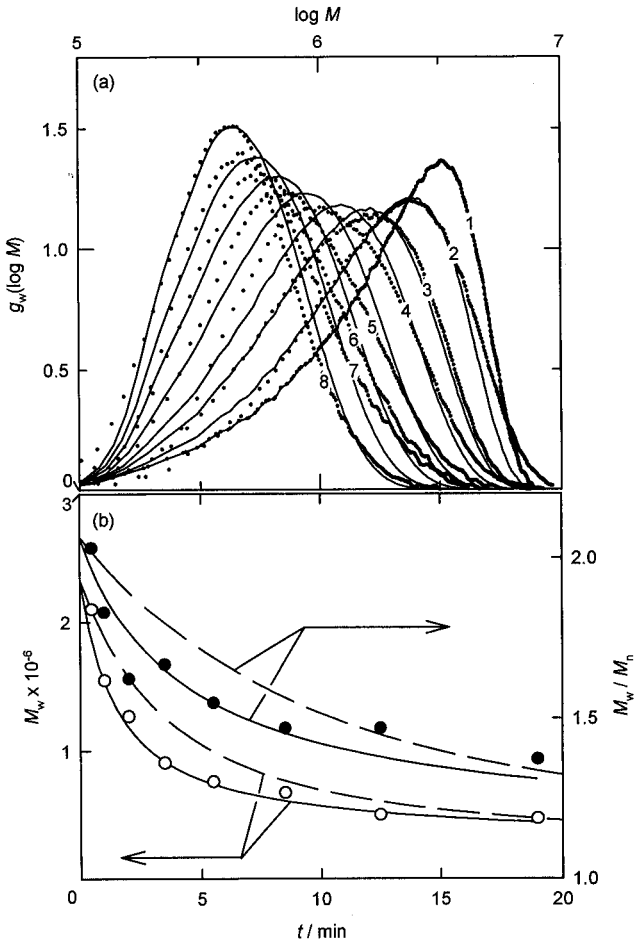

Figure 5. (a) Measured and simulated molecular weight distributions and (b) changes of the weight-average molecular weight M_w and the degree of polydispersity M_w/M_n in the ultrasonic irradiation process for $(A)_n{\cdot}2(I)_n$. (a) Dotted curves are GPC/LALLS-determined experimental molecular weight distributions. Irradiation time in min: (1) 1, (2) 1.5, (3) 2, (4) 3, (5) 4.5, (6) 6.5, (7) 9.5, (8) 13.5. Solid lines are simulated molecular weight distributions based on model V. The weight fraction $g_w(\log M)$ was plotted against the logarithm of molecular weight log$M$. (b) Circles are experimental values, M_w (○) and M_w/M_n (●). Solid lines are simulated on the basis of the modified newly proposed scission model (V′). Broken lines are calculated on the basis of the newly proposed scission model (V).

on the ordinate and at the same time ($t = 0 - d$) on the abscissa. In the present case, $(U)_n$ is taken as the reference sample ($DP_w = 960$ and $d = 0$ min). The shift factor d is 2 min for DNA from Figure 3a and 4.5 min for $(A)_n{\cdot}2(I)_n$ from Figure 5b. Thus, the efficiency of ultrasonic scission may be visualized by assuming the unsonicated, starting samples have nearly the same degree of polymerization.

Figure 6 shows the modified plot of DP_w of three different nucleic acids against the adjusted sonication time, which is displaced for the sonication process to start at $t = 0$, 2, and 4.5 min. For the measured period of sonication time, the successive reduction of chain length apparently depends on multiple strandedness of polymer sample. To obtain sonicated fragments of the same reduced DP_w values, the longest irradiation time is required for $(A)_n{\cdot}2(I)_n$. These results may be interpreted as revealing that the single-stranded $(U)_n$ is most susceptible to the sonication, followed by DNA, with the triple-stranded $(A)_n{\cdot}2(I)_n$ helix being most resistant to sonic scission.

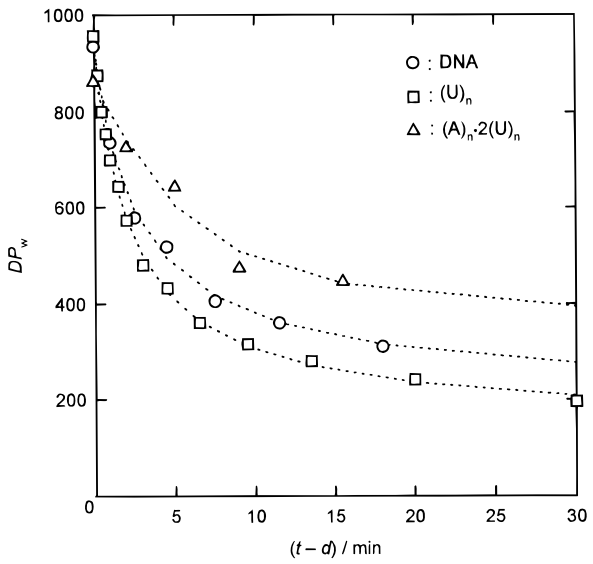

Figure 6. Comparison of changes in the weight-average degree of polymerization DP_w of DNA (○), $(U)_n$ (□), and $(A)_n{\cdot}2(I)_n$ (△) in the course of the sonication process. The abscissa is $t - d$, where t is time and d is an adjusting parameter (2 min for DNA, 0 min for $(U)_n$, and 4.5 min for $(A)_n{\cdot}2(I)_n$), to arrange the initial DP_w values approximately at the same starting point on the ordinate.

Comparison of Measured and Simulated Molecular Weight Distributions. The Case of DNA. Now the experimental data of the g_w vs M, M_w vs t, and M_w/M_n vs t curves are all compared with the results of simulation on the basis of the scission models cited in the previous section. The solid lines in Figure 2a−e represent the computer-aided simulation of g_w vs M curves for successively sonicated fractions, which are denoted with numerals. The no. 1 sample is the first 30-s irradiated fraction and taken as the reference for molecular weight distribution because of the reason cited (vide supra).

The distribution curves in Figure 2a were calculated on the basis of the random scission model (I). The measured distribution profiles become progressively narrower with the increase in distribution peaks, as the chain scissions proceed. The simulated curves, however, show narrowing, as observed experimentally, only at the initial stage but no further sharpening of breadth nor increase of the peak height at later stages. Thus, it is safe to conclude that the random scission model fails to describe the sonication mechanism of DNA, except only for the initial stage.

The calculated results in Figure 2b are based on the midpoint scission model (II). The simulated distributions curves become progressively narrower with higher peaks, as the sonication time is increased. The fitting to measured profiles is slightly improved in the lower molecular weight region, indicating that the lower molecular weight DNA may be sheared in the middle of the double strands. The calculated results in Figure 2c are based on the gaussian scission model (III), in which the standard deviation, σ, of the Gaussian function is set to be $^2/_{10}$ of the chain length. The fitting of measured distribution profiles with this model is still unsatisfactory, though it is better than the two previous models I and II. The Gaussian model is also concluded to be inconsistent with the experimental DNA scission process.

The calculated g_w vs M curves in Figure 2d are based on the classical scission model (IV), which predicts that

the chain is randomly sheared in the middle region but both ends remain resistant to sonication. In this calculation, the end molecular weight inaccessible to shearing (cf. M_0 in Figure 1) was assumed to be 1.5×10^5 for the best fitting. The distribution curves simulated for the later sonication stages become irregular at the lower molecular side, where sharp and anomalous peaks appear. In conclusion, this classical model is also inadequate for the scission mechanism of DNA chains.

The calculated curves in Figure 2e are based on the newly proposed model (V), for which values of M_0 and n are best assumed to be 1.5×10^5 and unity, respectively. By using this model, the measured distribution profile of each fraction can be reproduced superbly well in the entire course of sonication as regards the breadth and the peak position. According to model V, the molecular weight distribution for polymer chains higher than 3×10^5 in M_w-values, generally changes in a manner as predicted by model I, but the pattern shifts to another mechanism, as predicted by model II for chains shorter than 3×10^5. Thus, the newly proposed model (V) includes both models I and II as the limiting case and is no doubt the best possible mechanism for explaining the ultrasonic scission process of DNA.

Now the simulated results for the dependence of M_w and M_w/M_n values on the sonication time is discussed. In Figure 3a, the M_w vs t curves, computed according to models I−V′, are compared with experimental data (circles). Both models I and II fail to reproduce the dependency, whereas models III−V apparently reproduce the general tendency; however, none of the simulated curves fit the observed points. Therefore, model V must be modified slightly by taking into account the number concentration of polymers in the system. This model is designated as model V′, in which the scission probability **A** in eq 3 is now modified as

$$\mathbf{A} = \frac{1}{{c_n}^m}\begin{pmatrix} a(1,1) & a(1,2) & \cdots & a(1,n) & \cdots \\ a(2,1) & a(2,2) & \cdots & \cdot & \cdot \\ \cdot & \cdot & \cdots & \cdot & \cdot \\ \cdot & \cdot & \cdots & \cdot & \cdot \\ a(n,1) & \cdot & \cdots & a(n,n) & \cdots \\ \cdot & \cdot & \cdots & \cdot & \cdot \end{pmatrix} \quad (10)$$

where ${c_n}^m$ is the ratio of numbers of sonicated polymers to those unsonicated in the original sample with an adjustable parameter m. It should be noted that this modification affects only the dependence of molecular weight distribution on the time, i.e., the rate of change, but not the shape of the distribution profile. As shown in Figure 3a with the solid line, the simulated curve fits to the measured data excellently in the entire course of sonication. In the case of DNA, the parameter m in eq 10 is taken to be $^1/_3$ for the best fitting, the physical meaning being open for future work.

In Figure 3b, the simulated dependence of the polydispersity of sonicated fractions on sonication time t is compared with the experimental data. Values of M_w/M_n calculated on the basis of model I increase with a lapse of sonication, contrary to the data. The simulation with model II is also distinctly off the measured values, whereas model IV yields an anomalous dependence (not shown in Figure 3b), because of the abnormal behavior of g_w vs M profiles (cf. Figure 2d). The M_w/M_n vs t curves, simulated with models III, V, and V′, all agree with the measured data reasonably well. Considering large experimental uncertainties, the newly proposed model (V) and its variation (V′) are again proved to be the best for the sonic scission of DNA.

The Case of $(U)_n$. In Figure 4a, the simulated g_w vs M curves are compared with the experimental data for single-stranded $(U)_n$. The distribution profiles were calculated on the basis of model V with two parameters, $M_0 = 1.0 \times 10^5$ and $n = 2$. Since these calculated distribution profiles are in excellent agreement with measured ones, it is concluded that model V can describe the sonication process of $(U)_n$. It should be noted that the other models I−IV are unable to reproduce measured distribution profiles for the entire course of sonication (not shown). Thus, the scission process of $(U)_n$ resembles that of DNA. The $(U)_n$ chain is hardly sheared at end portions, where molecular weights are less than 1×10^5, but can be sheared randomly in the middle portion; the end portion of DNA is slightly less scissile ($M_0 = 1.5 \times 10^5$). The scission probability of the end portion for $(U)_n$ ($n = 2$) is lower than for DNA ($n = 1$), indicating that the domain between the scissile middle and unscissile end regions is more distinct for $(U)_n$ than for DNA. These subtle differences may stem from the differing structural rigidity of single- and double-stranded nucleic acid conformations.

In Figure 4b, the change of M_w and M_w/M_n with sonication time is shown. The simulation was carried out, by using model V′, for which $m = 0$ in eq 10. Measured points of both M_w and M_w/M_n fit to the simulated curves quite well over the entire course of sonication. The scission probability of $(U)_n$ does not depend on the (number) concentration, whereas that of DNA depends on this concentration.

The Case of $(A)_n \cdot 2(I)_n$. In Figure 5a, the simulated molecular weight distribution profiles of $(A)_n \cdot 2(I)_n$ are compared with the experimental data. The simulation was carried out, by using model V with parameters M_0 ($=1.7 \times 10^5$) and n ($=5$). The agreement between these two sets of profiles is excellent for the entire sonication process. When other models were employed for simulation, the agreement was less satisfactory. Thus, it can be concluded that the sonication of triple-stranded $(A)_n \cdot 2(I)_n$ also proceeds according to the newly proposed model (V). The parameter n of 5 indicates that the end portions are clearly distinguishable from the middle portion of the polymer chain.

In Figure 5b, the observed dependence of M_w and M_w/M_n on sonication time is simulated with model V′, the modified new model, by taking into account the increase in the number of polymer chains as produced by successive scissions and also by assigning a value of 0.5 to the parameter m in eq 10 (solid-line curves). For comparison, another set of simulation was performed on the basis of model V without considering the parameter (i.e., $m = 0$), the result being given with dashed curves. The excellent agreement between measured values and simulated curves strengthens the proposed mechanism (model V′) for the sonication process of $(A)_n \cdot 2(I)_n$.

Conclusion

The ultrasonic irradiation of DNA, $(U)_n$, and $(A)_n \cdot 2(I)_n$ successively reduces the molecular weight in solution, making the molecular weight distribution progressively narrower, regardless of their different structures. The sonication process can be explained satisfactorily with the scission model newly proposed in the present work. This model assumes that the high molecular weight polymer chain is sheared randomly in the middle portion but is hardly scissile in the end regions. The joining domain is distinct in the order $(A)_n \cdot 2(I)_n >$ DNA

> $(U)_n$. These unscissored ends correspond to the fraction of shortest fragments, yielding the limiting low molecular weight products by careful sonication (DP ≒ 160 for $(A)_n \cdot 2(I)_n$, 230 for DNA, and 300 for $(U)_n$). Thus, the purpose of preparing well-fractionated nucleic acid samples of various conformations in a large (gram order) quantity for physicochemical studies in solution is now achieved.

Acknowledgment. We thank Mr. N. Takata of this laboratory at Hiroshima University for his kind supply of the sonication data of DNA. This work was in part supported by Grant-in-Aid for Developmental Scientific Research (B) 06554031 (K.Y.) from the Ministry of Education, Science and Culture, Japan.

References and Notes

(1) Doty, P.; McGill, B. B.; Rice, S. A. *Proc. Natl. Acad. Sci. U.S.A.* **1958**, *44*, 432.
(2) Freifelder, D.; Davison, P. F. *Biophis. J.* **1962**, *2*, 235.
(3) Hughes, D. E.; Nyborg, W. L. *Science* **1962**, *138*, 108.
(4) Richards, O. C.; Boyer, P. D. *J. Mol. Biol.* **1965**, *11*, 327.
(5) Pritchard, N. J.; Hughes, D. E.; Peacocke, A. R. *Biopolymers* **1966**, *4*, 259.
(6) Obrenovitch, A.; Aubel-Sadron, G. *J. Chim. Phys.-Chim. Biol.* **1971**, *68*, 521.
(7) Londos-Gagliardi, D.; Serros, G.; Aubel-Sadron, G. *J. Chim. Phys.-Chim. Biol.* **1971**, *68*, 666.
(8) Londos-Gagliardi, D.; Serros, G.; Aubel-Sadron, G. *J. Chim. Phys.-Chim. Biol.* **1971**, *68*, 670.
(9) Record, M. T., Jr.; Woodbury, C. P.; Inman, R. B. *Biopolymers* **1975**, *14*, 393.
(10) Bertazzoni, U. *Biochim. Biophys. Acta* **1975**, *395*, 239.
(11) Godfrey, J. E. *Biophys. Chem.* **1976**, *5*, 285.
(12) Godfrey, J. E.; Eisenberg, H. *Biophys. Chem.* **1976**, *5*, 301.
(13) Davis, A. W.; Phillips, D. R. *Biochem. J.* **1978**, *173*, 179.
(14) Charney, E.; Yamaoka, K. *Biochemistry* **1982**, *21*, 834.
(15) Fukudome, K.; Yamaoka, K.; Nishikori, K.; Takahashi, T.; Yamamoto, O. *Polym. J.* **1986**, *18*, 81.
(16) Fukudome, K.; Yamaoka, K.; Ochiai, H. *Polym. J.* **1987**, *19*, 1385.
(17) Tanigawa, M.; Mukaiyama, N.; Shimokubo, S.; Wakabayashi, K.; Fujita, Y.; Fukudome, K.; Yamaoka, K. *Polym. J.* **1994**, *26*, 291.
(18) Fukudome, K.; Yamaoka, K.; Yamaguchi, M. *Polym. J.* **1990**, *22*, 937.
(19) Yamaoka, K.; Fukudome, K. *J. Phys. Chem.* **1990**, *94*, 6896.
(20) Fukudome, K.; Kumamoto, Y.; Yamaoka, K. *Polym. J.* **1995**, *27*, 101. Also see references cited therein.
(21) Montroll, E. W.; Simha, R. *J. Chem. Phys.* **1940**, *8*, 721.
(22) Jellinek, H. H. G.; White, G. *J. Polym. Sci.* **1951**, *6*, 745.
(23) Mostafa, M. A. K. *J. Polym. Sci.* **1956**, *22*, 535.
(24) Saito, O. *J. Phys. Soc. Jpn.* **1958**, *13*, 198.
(25) Kotliar, A. M.; Anderson, A. D. *J. Polym. Sci.* **1960**, *45*, 541.
(26) Kotliar, A. M.; Podgor, S. *J. Polym. Sci.* **1961**, *55*, 423.
(27) Okuyama, M.; Hirose, T. *J. Appl. Polym. Sci.* **1963**, *7*, 591.
(28) Inokuti, M. *J. Chem. Phys.* **1963**, *38*, 1174.
(29) Heymach, G. J.; Jost, D. E. *J. Polym. Sci.* **1968**, *C25*, 145.
(30) Ballauff, M.; Wolf, B. A. *Macromolecules* **1981**, *14*, 654.
(31) Jellinek, H. H. G.; White, G. *J. Polym. Sci.* **1951**, *6*, 757.
(32) Thomas, J. R. *J. Phys. Chem.* **1959**, *63*, 1725.
(33) Shaw, M. T.; Rodriguez, F. *J. Appl. Polym. Sci.* **1967**, *11*, 991.
(34) Zimm, B. H. *J. Chem. Phys.* **1948**, *16*, 1099.
(35) Yamaoka, K.; Suzuto, M., manuscript in preparation.

MA9603701